Materials Research Bulletin 192 (2025) 113561

Contents lists available at ScienceDirect

Materials Research Bulletin

journal homepage: www.elsevier.com/locate/matresbu

Research Papers

Extracting High Purity Nano-silica from Oil Shale: Valorising a Neglected Natural Resource

Anas Krime [a,b,c], Miriam Rita Eloufir [a], Sanaâ Saoiabi [a], Mouhaydine Tlemcani [b,c,*], Manuela Morais [b,c], Ahmed Saoiabi [a]

[a] Laboratory of Applied Chemistry of Materials, Department of Chemistry, Faculty of Sciences, Mohammed V University in Rabat 10090, Morocco
[b] Instrumentation and Control Laboratory-LAICA, Center for sci-tech Research in Earth system and Energy – CREATE University of Evora, 7000-671, Evora, Portugal
[c] Laboratory of Water, Center for sci-tech Research in Earth system and Energy – CREATE University of Evora, 7000-671, Evora, Portugal

ARTICLE INFO

Keywords:
Moroccan oil shale
Neglected resource
Silica nanoparticles
Amorphous
High-purity

ABSTRACT

Silica nanoparticles are indispensable materials in modern industries because of their versatility. However, conventional production sources are intensive and environmentally burdensome. Given these considerations, this manuscript presents a novel, abundant, and inexpensive natural resource for extracting high-purity nano-silica. Indeed, a chemical extraction method was applied to a neglected Moroccan oil shale. The synthesized silica nanoparticles were thoroughly characterized using a range of analytical techniques. The nitrogen adsorption-desorption isotherms exhibited a Type IV profile with a surface area of 381.0582 m^2/g, X-ray diffraction (XRD) confirmed its amorphous structure with a broad peak centered at $2\theta \approx 22.5^\circ$, while energy-dispersive X-ray spectroscopy-mapping (EDX-mapping) validated the exceptional purity reaching up to 99.99 %. Additionally, scanning and transmission electron microscopy (SEM and TEM) revealed dense agglomerates of nanoparticles ranging from 9 to 15 nm in diameter. Fourier-transform infrared spectroscopy (FTIR) indicated the presence of silanol (Si–O–H) and Siloxane (Si–O–Si) characteristic bands, indicating the formation of silica. Thermal analysis (DSC and TGA) demonstrated the thermal stability of the mesoporous structure up to 900 °C and the presence of both physically adsorbed and chemically bound water. This high yield of silica (92 %) makes this underexploited oil shale resource commercially viable for large-scale applications in catalysis, water treatment, and nanotechnology. Environmentally, the process promotes waste valorization by transforming shale byproducts into amorphous nano-silica and supports circular economy principles, enabling developing economies to locally produce advanced materials with minimal ecological impact.

1. Introduction

Silica is one of the most prevalent elements found on Earth and in the lithosphere, due to their availability and environmental friendliness [1]. Its versatile applications span various fields, including the manufacturing of glasses, optical fibers, food additives, as well as its use in battery electrode materials, absorbents, drugs, catalysis, cosmetics, agriculture (to enhance germination and stress resistance) [2]. Moreover, silica nanoparticles are known for their unique physicochemical characteristics, including high surface area and good thermal and mechanical stability, which lead them to enhance charge separation [3], improve the molecular interaction and selective binding [4]. When it is combined (doped or coated) with other metal oxides such as Titanium oxide (TiO_2), Zinc oxide (ZnO), and iron oxide (Fe_3O_4), their properties are significantly enhanced, making these composites efficient for photocatalytic, antimicrobial, and other environmental applications [5]. This position it to hold a key role in industry covering a range from ceramic to advanced nanotechnology.

Natural traditional sources such as quartz sand necessitate significant energy input for mineral purification and maintaining elevated temperatures [6]. It can also be obtained from chemicals like tetraethyl orthosilicate (TEOS) or tetramethyl orthosilicate (TMOS), which are both toxic and expensive (<$600/ton) [7]. Additionally, alternative biomass like rice husk [8], bamboo sticks, sugar cane bagasse, wheat straw [9] can be used as a precursor for the synthesis of nano silica while this production reduces their economic value due to their increase demand for biofuel, bioenergy, soil enhancement. From investors view point, profitability in stability and competitive yield is top priority to

* Corresponding author.
E-mail address: tlem@uevora.pt (M. Tlemcani).

https://doi.org/10.1016/j.materresbull.2025.113561
Received 27 January 2025; Received in revised form 17 May 2025; Accepted 20 May 2025
Available online 23 June 2025
0025-5408/© 2026 The Authors. Published by Elsevier Ltd. This is an open access article under the CC BY license (http://creativecommons.org/licenses/by/4.0/).

find sustainable alternative sources [10].

In this context, Therefore, Moroccan oil shales emerge as a viable, neglected, and highly abundant natural resource distributed across three structural domains in the kingdom: the Raffin domain (Arbaa Ayacha and region), the Atlastic domain (Timahdit), and the Atlantic basin (Tarfaya) [11]. Morocco holds the sixth position worldwide in terms of substantial oil shale reserves, boasting an estimated 53 billion barrels of oil. This places it just behind the USA, Russia, the Democratic Republic of the Congo, Brazil, and Italy in the global ranking [12]. Oil shale, being a sedimentary rock, is primarily comprised of organic matter, mineral components, and water. The pivotal organic element, kerogen, constitutes a complex mixture of organic compounds convertible into oil and gas. Additionally, oil shale harbors various minerals, including silica, commonly found in many deposits, often in the form of quartz, with a percentage exceeding 84 % [13]. The composition of oil shale varies depending on geological and environmental conditions, and it has been used as a mineral precursor in a variety of industries, including the manufacture of various chemical products, ammonium bituminosulfonate, a material additive for tile, brick, and pottery, and a low-cost source of alumina for Portland cement. Harnessing this source proves beneficial not only due to its economic feasibility but also because it not utilized for food production or energy like agriculture biomass. This, in turn, opens avenues for producing high-purity silica at a lower cost [14].

Several studies have explored the extraction of nano-silica from diverse sources. Park et al. detailed a sequential two-stage recovering method involving mechanical milling followed by treatment with alkaline solutions, achieving a silica yield of 89 % and a purity of 99.99 %. However, this approach resulted in a reduced surface area of 1.973 m^2/g [15]. Using a hydrothermal method, Ganguli and Ganguly produced nanosilica particles with a specific surface area of 119 m^2/g [16]. YING-MEI et al. produced amorphous silica with a 150 m^2/g surface area from Huadian oil shale waste (China) using an alkali-extraction process [17]. Durairaj et al. created silica nanoparticles (SiNp) from Bambusa vulgaris leaf ash using the sol-gel process, getting a specific surface area of 60.40 m^2/g [18]. Amorphous SiO_2 with a specific surface area of 116 m^2/g was prepared from unleached rice husk by Rohani et al. [19]. G. Falk et al. synthesized silica nano-particles derived from bagasse obtained from sugarcane ash using a sol-gel polymer approach (process 1) and a thermal process followed by acid leaching treatment (process 2), achieving surface areas of 124.89 m^2/g and 8.28 m^2/g, respectively [20]. Pillai et al. used Hydrochloric acid (HCl) leaching to extract silica from rice husks, resulting in a superficial area of 48.9 m^2/g [21]. Sachan et al. used a simple chemical approach to synthesize silica nanoparticles from leaf biomasses of Saccharum ravannae (SRL), Saccharum officinarum (SOL), and Oryza sativa (OSL) with total surface areas of 39,989 m^2/g, 9555 m^2/g, and 178.11 m^2/g [22].

This research introduces a novel approach to extract silica nanoparticles from Moroccan oil shale as an alternative source to respond to the urgent demand for a raw material [23]. Capitalizing on the abundant availability and remarkable properties (stable and abundant) of Moroccan oil shale, the current study focuses on producing valuable nanosilica through a resource-efficient procedure. In contrast to alternative biomass feedstock, our underutilized mineral resource demonstrates a scalable solution to the development needs for advanced nanomaterials and the industrial valorization of unutilized local resources. This endeavor aims to position Moroccan oil shale silica as a competitive product capable of meeting the requirements for high-performance applications across various fields.

To further understand the main physicochemical features, the samples were evaluated utilizing a number of methods. Techniques used for analysis included Brunauer-Emmett-Teller and Barrett-Joyner-Halenda (BET-BJH), Scanning Electron Microscope combined with Energy Dispersive X-ray-mapping (SEM/EDX-mapping), Differential Scanning Calorimetry (DSC), Thermogravimetric Analysis (TGA), Transmission Electron Microscope (TEM), Fourier Transform Attenuated Total Reflectance (FTIR-ATR) and X-ray Diffractometry (XRD).

2. Experimental section

2.1. Reagents and chemicals

Inorganic acid hydrochloride (HCl) and sulfuric (H_2SO_4), sodium hydroxide (NaOH) were acquired from Carlo Erba Reagents (Table 1) and used in the current investigation without further purification. Throughout the experiment, Whatman No 41 filter paper and distilled water were used.

2.2. Extraction of silica nanoparticles from Moroccan oil shales

In this work, we have chosen a productive and economical process [24] for the extraction of silica gel from the oil shale that is located in the area of Arbaa Ayacha. The shale in this area is characterized by a high percentage of SiO_2, as demonstrated by our laboratory team [13], which reached a concentration of 84 %. This value far exceeds that found in other locations.

The silica extraction process initiates with the pretreatment of oil shales. The sample undergoes a series of steps, including crushing, grinding, washing, and sieving, to attain particles within the 100 to 40 μm range. Following these steps, the processed sample is calcined at 550 °C for 5 h to help break down its organic components.

The calcined oil shale (15 g) was then combined with 150 ml of sodium hydroxide (NaOH) (12 %) solution in a three-necked flask. It was then stirred magnetically for 6 h to try to dissolve the silica at a constant temperature of 100 °C, resulting in the creation of sodium silicate as indicated in reaction 1:

$$SiO_2 + 2NaOH \rightarrow Na_2SiO_3 + H_2O \quad (1)$$

The resulting suspension was then filtered through Whatman No 41 ash-free filter paper and washed with hot distilled water before cooling. The pH of the filtrate was adjusted to 7 by continuous spinning in a 13 % of sulfuric acid (H_2SO_4) solution. The synthetic hydrogel, which was white and soft to the touch, was allowed to cool to room temperature. It was then filtered and washed with distilled water to remove the remaining sulfate salt according to the reaction (2). The solid residue was dried overnight.

$$Na_2SiO_3 + H_2SO_4 \rightarrow SiO_2 + Na_2SO_4 + H_2O \quad (2)$$

Following that, the powder was refluxed with a diluted hydrochloric acid (HCl) (3,5 %) solution for 1 hour was used to purify the silica by the removal of soluble minerals such as Al, Ca, Fe and magnesium. The suspension was then filtered and carefully washed with distilled water. Calcination at 800 °C for two hours in a muffle furnace was the final element of the process, which resulted in the production of fine white silica powder. The morphological and elemental properties of the final silica nanoparticles have been rigorously investigated using a range of instruments.

The percentage yield of silica nanoparticles derived from Arbaa Ayacha oil shales was determined using the formula [25]:

$$Wt.\% = (massofsilicananoparticles / massofusedO.A.A) \times 100$$

The extracted yield of silica nanoparticles was found to be more than 92 ± 0.5 %. Furthermore, Energy dispersive X-ray spectroscopy (EDX)

Table 1
Properties of chemical reagents.

Product Name	Formule moléculaire	Country of Origin	Purity	Manufacturer
Hydrochloric Acid	HCl	France	37 %	Carlo Erba Reagents
Sulfuric Acid	H_2SO_4		96 %	
Sodium Hydroxide	NaOH		98 %	

was used to measure the pureness of the nano-bio-silica sample. In particular, no remarkable peaks for other metals were observed (Fig. 4 (S_1)), demonstrating the effectiveness of the simple extraction process in generating highly pure nano-silica from Moroccan oil shales.

2.3. Characterization of samples

Sample characteristics are provided in the in the main text and figures.

3. Results and discussion

3.1. Brunauer–Emmett–Teller (BET) surface area analysis

Fig. 1 illustrates both the nitrogen physisorption data recorded at 77 K for untreated oil shale and extracted nano-silica, and the distribution of pore sizes estimated from a desorption isotherm using The BJH analysis method. Isotherms have a typical IV shape with a type H1 loop, suggesting a cylindrical pore size distribution and a mesoporous structure for the silica, in contrast to the significant microporosity observed in the Arbaa Ayacha shale [26], as classified by the IUPAC criteria [27]. The bio-silica particles have an effective area of 381.05 m^2/g and an average pore size of approximately 82.22 Å, whereas the Arbaa Ayacha oil shale has a much lower surface area of 5.7931 m^2/g. As shown in the Table 2, the surface area of our nanobiosilica has a higher surface area than commercial silica (172 m^2/g) and other silica produced from different sources.

3.2. Fourier-transform infrared spectroscopy (FTIR)

Fig. 2 shows the typical FTIR spectrum of a raw AA sample and the isolated nano-silica particles. Significant bands around 1125–890 cm^{-1} and 810–450 cm^{-1}, relating to the mineral component, quartz, can be seen in Fig. 2(S_0). The narrow band at 1117 cm^{-1} confirms the presence of silicon dioxide, which is the highest concentration of silicon dioxide in oil shale. Fig. 2(S_1) shows absorption bands at 456 cm^{-1}, 810 cm^{-1} and 1117 cm^{-1} characteristic of SiO_2 [35,36]. Si-O-Si bending vibrations cause the sharp band at 456 cm^{-1} [37]. The adsorption band around 810 cm^{-1} is formed by the symmetry vibrations of the siloxane moieties towards (Si-O-Si), while the band around 922 cm^{-1} is related to the Si-O stretching vibration of the silanol group [38]. Asymmetric vibrations of Si-O-Si in silica are responsible for the presence of a broad band at 1117 cm^{-1} [39]. The elimination of hydroxyl or organic groups in the densely packed powder is indicated by the absence of the O—H stretching and

Table 2
Surface specific area, synthesized method and purity of silica from various sources.

Source	Method	Surface area m^2/g	Purity %	Reference
Rice husk Ash	Sol-gel	78	98	[28]
Bamboo leaves	Pyrolysis followed by alkaline extraction	328	98.26	[29]
Sugarcane Bagasse Ash	Sol-gel	240	98.92	[30]
Rice Husk	Acid leaching + calcination	234.25	99.99	[31]
bamboo leaf ash	Sol-gel	159.224	94.2	[32]
Commercial silica	Acid neutralization of sodium silicate	172	99.99	[1]
Industrial silica	–	301.21	high	[33]
Rice husk	Acid leaching	129.12	98.87	[5]
Rice husk	Microwave leaching	84.56	98.8	[34]
Morocan Oil shale	Sol-gel	381.058	99.99	This study

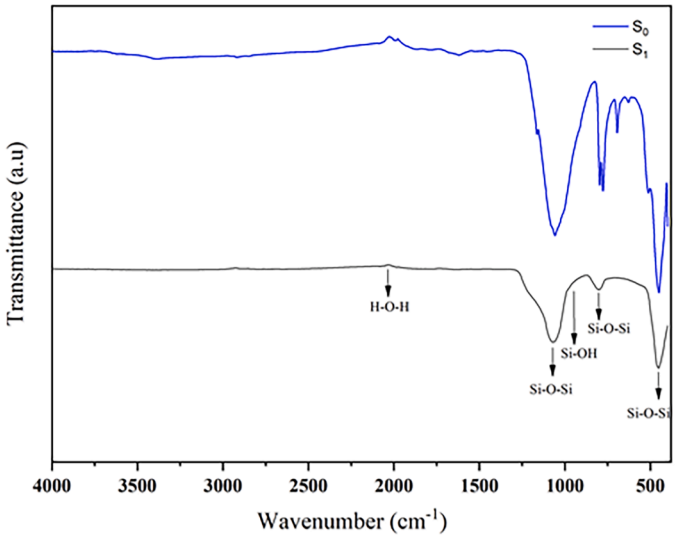

Fig. 2. FTIR of the studied rock sample (S_0) and amorphous silica (S_1).

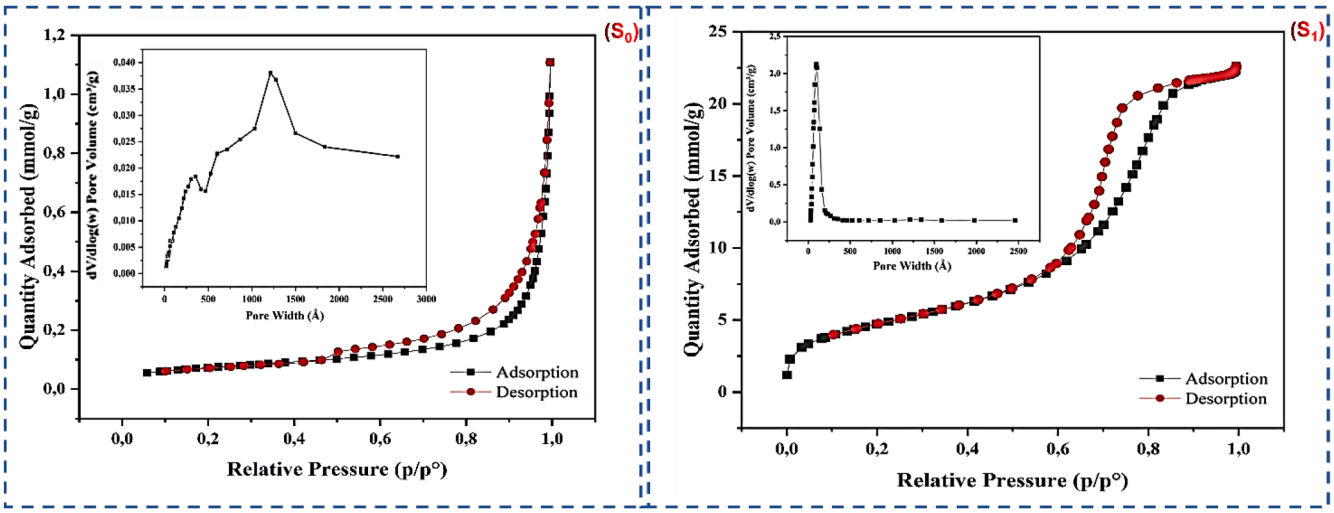

Fig. 1. Relative pressure vs adsorbed amount of oil shale Araba Ayachaa (S_0) and nano silica S_1 (SiO_2).

bending modes in the absorption band region at 3448 and 1635 cm^{-1} [40].

3.3. X-Ray diffraction analysis (XRD)

Fig. 3 depicts the patterns identified by XRD of oil shale from Moroccan Rif (Arbaa Ayacha area) with extracted silica. The X-ray powder diffractogram shows that the major constituent of the bituminous rock sample is quartz including traces of other minerals such as illite (at theta = 20, 34, 36 and 63°), pyrite (at theta = 27 and 40°) and chlorite (at theta= 25°) [41]. The intense broad band which starts from the two-theta region 15° and ends in 30° indicates the amorphous nature of the silica [5] obtained from the oil shale. The high purity of the silica produced is also confirmed by the absence of any other strong peaks [42].

3.4. SEM - EDX and mapping analysis

Fig. 4 illustrates the surface morphologies of the crude oil shale sample and the silica nano-powder. The SEM micrographs in Fig. 4(S_1) show the effectiveness of the silica extraction method. The majority of the SiO_2 particles had a spherical shape with a reasonably uniform size on the surface, as well as a homogeneous distribution and little agglomeration [43]. Despite the acidic treatment, the morphology of silica nanoparticles remained indicted. In contrast, in Fig. 4(S_0), the micrograph of the bituminous rock sample revealed to have large particles with different sizes, including irregular particle shapes, which are widely distributed on the surface [44].

The EDX spectra of the studied material (Fig. 4, Table S_0) show peaks for Si, Al, Fe, Mg, S, K, Ca, Zn, and oxygen. The results confirm silica (SiO_2) as the major element, indicating that the chemical composition of the Moroccan oil shale surface is dominated by quartz species due to the high concentrations of Si and O. Furthermore, the silica powder contains 44.55 wt % silicon and 55.45 wt % oxygen with an O/Si molar ratio of 2.18 according to the EDX measurement (Fig. 4, Table S_1), which corresponds to the stoichiometric ratio of natural silica [45]. The above-mentioned result also confirms the absence of other elements indicating that the acidic treatment is beneficial in removing all minerals and impurities from the silica. This may be because silica is insoluble in acids and remains intact, while the Fe, Al, and traces of alkali metals dissolve in the dilute solution, indicating the formation of an exceptionally pure silica structure [46].

The Fig. 5 confirms the stoichiometric ratio of S_1 and exhibits a uniform distribution of silicon and oxygen, indicating the high purity and good homogeneity of the extracted silica (S_1).

3.5. Transmission Electron Microscope (TEM) analysis

Fig. 6 shows the TEM image of the silica sample, showing that the nano-bio-silica particles are spherical. The agglomeration of the particles is particularly noticeable, which is related to the hydrogen bonding between the surface OH groups inside the silica molecules [47]. A similar TEM image was also presented by [1]. Discrepancies in particle distribution, evident from SEM images, are mirrored in the TEM image. These irregularities in particle morphology contribute to the silica's amorphous nature, consistent with findings by Mor et al. [22]. The amorphous state previously identified through XRD analysis is reaffirmed here. The extracted silica particles exhibit diameters in the nanometric range, typically ranging from 9 to 15 nm.

3.6. Differential scanning calorimetry (DSC) analysis

The morphological study of the SEM images shows that the nano-silica exhibits agglomeration, which is temperature-dependent. DSC analysis is used to investigate the thermal behavior of S_1 nanoparticles at temperatures ranging from 25 to 800 °C (Fig. 7). An exothermic peak at 65 °C and an endothermic peak at 92 °C are shown in Fig. 7(b). The evaporation of water molecules from the surface silanol groups and their subsequent degradation cause these peaks [48]. The DSC curve of S_0 shows three exothermic peaks at 115 °C, 245 °C, and 596 °C, and three endothermic peaks at 376 °C, 522 °C, and 627 °C. The endothermic peak at 115 °C, which begins at 100 °C, is most likely caused by dehydration, or the loss of physisorbed surface moisture from Arbaa Ayacha shales. The decomposition of organic matter and dehydroxylation of metallic hydroxyls are responsible for the exothermic peak at 245 °C and the endothermic peak at 376 °C, respectively. Finally, the mineral composition and combustion resistance of organic molecules in these geological materials may be responsible for the endothermic peaks at 522 °C and 627 °C and the exothermic peak at 596 °C.

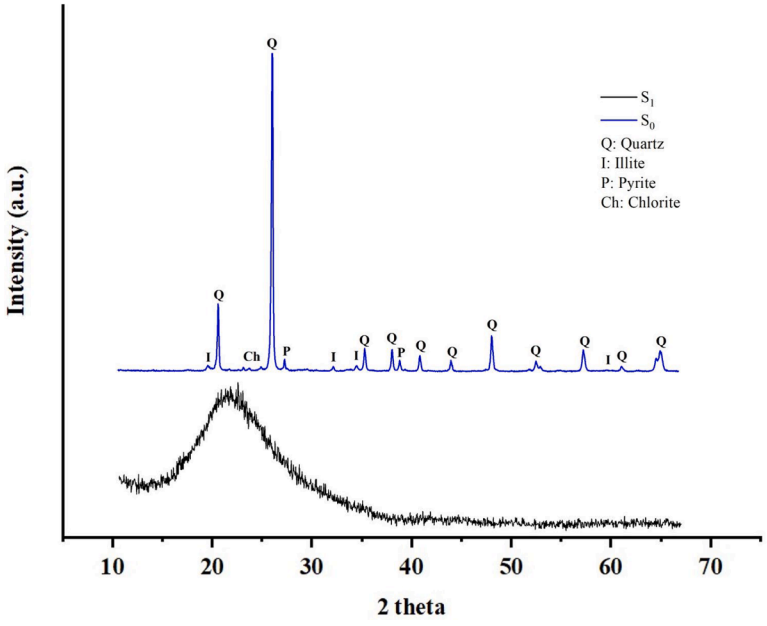

Fig. 3. X-ray diffractograms of the studied sample (S_0) and silica powder (S_1).

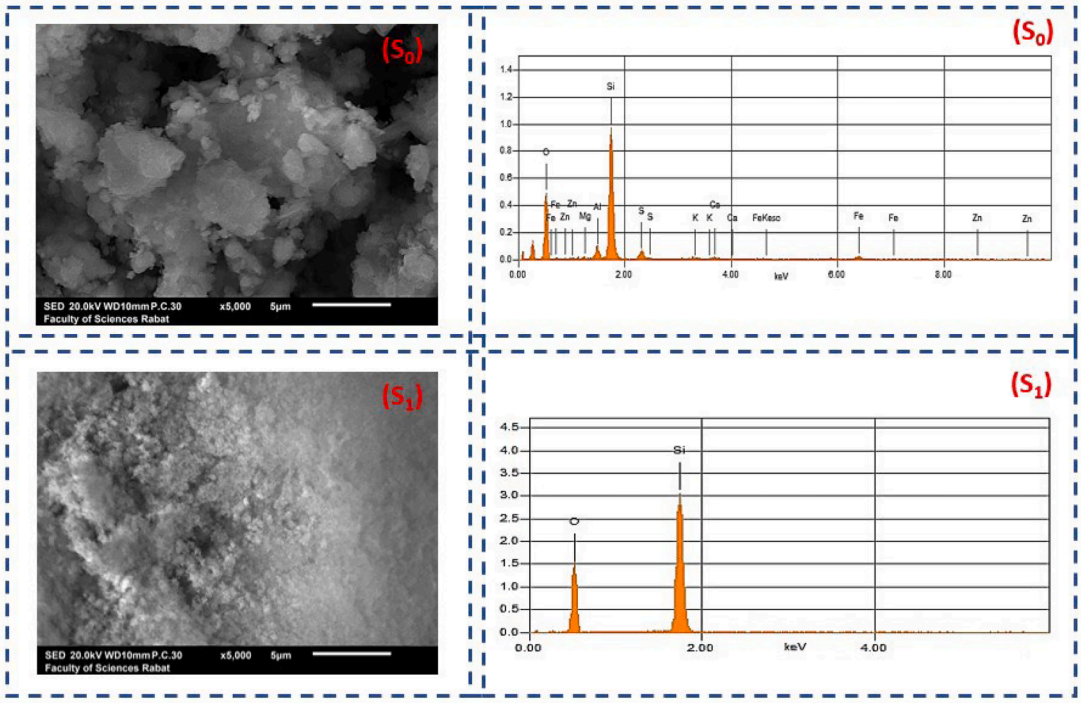

Fig. 4. SEM and EDX micrographs of raw AA oil shale (S_0) and silica nanoparticles (S_1).

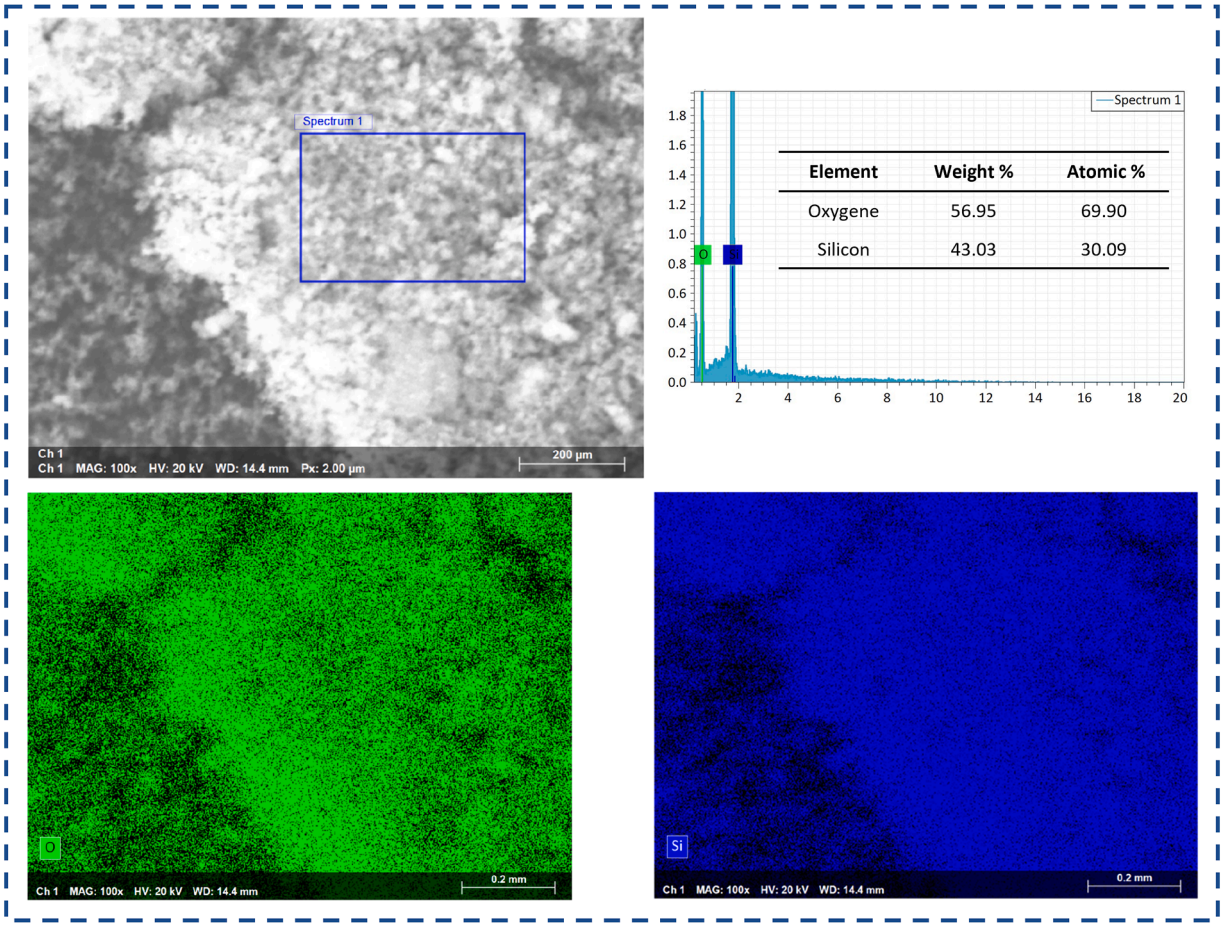

Fig. 5. SEM and EDX/Mapping of S_1.

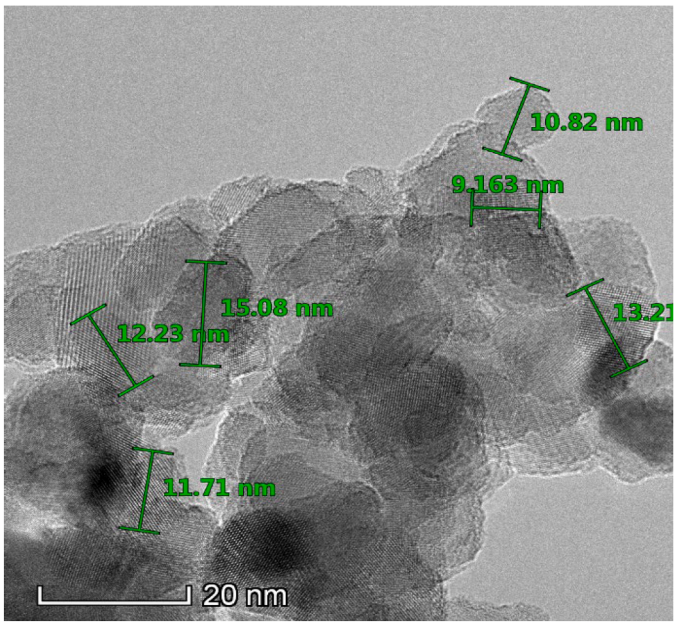

Fig. 6. TEM image of SiO_2 NPs.

3.7. Thermogravimetric analysis

Two of the most commonly used methods for determining the thermal properties of crystalline and amorphous materials are Differential Scanning Calorimetry (DSC) and Thermogravimetric Analysis (TGA). While DSC monitors the energy absorbed or released by a sample when heated or cooled, TGA records the change in weight of the sample under the same conditions. TGA is often used to complement DSC analysis in assessing thermal stability [49].

In this study, the thermal stability of two samples, S_0 and S_1, was evaluated using TGA, as shown in Fig. 8. The results indicate that silica nanoparticles (S_1) exhibit greater thermal stability compared to Arbaa Ayachaa shales (S_0), with S_1 losing only 0.6 % of its weight at 200 °C, while S_0 loses 3 % at the same temperature. This difference in thermal stability is consistent with the findings from DSC analysis. The significant weight loss in the raw oil shales can be attributed to the evaporation of water molecules. Additionally, S_0 exhibits weight losses of about 10.3 % between 200–450 °C and 450–900 °C, likely due to the decomposition of organic groups and their resistance to combustion [23]. Consequently, the study suggests that bio-nanosilica is suitable for high-temperature applications, thanks to the high-temperature resistance provided by the capping and stabilizing agents around the amorphous silica [50].

3.8. Measurement of pH_{pzc}

The point zero charge pH (pH_{PZC}) of the adsorbent was determined using the pH salt technique, which has been tested by several researchers [51,52]. In this study, the pH_{PZC} of the adsorbent was determined by adding 20 mL of Sodium chloride (0.05 M) and drops of hydrochloride acid and sodium hydroxide (0.1 M) to each flask to change the initial pH (pHi) before adding 20 mg of adsorbent. The suspensions were shaken at 298 K for 48 h until equilibrium was reached. The collected samples were then filtered to obtain the final pH values (pH_f). An overview of the negative and positive aspects of the adsorbent surface is provided by measuring the point of zero charge (pH_{PZC}) [53]. PH_{PZC} represents the pH at which the surface charge is zero. It also provides information on the pH range that can be used for adsorption of cationic or anionic species, which plays an important role in the sorption process, especially when electrostatic forces are present. The pH_{PZC} value is determined by the intersection of the plot of final pH_f versus initial pH_0 [54]. The point zero charge of our adsorbent was 8.01 according to Fig. 9. Below this threshold ($pH_{PZC} > pH$), the surface of the SiO_2 will be positively charged because it will be protonated by the H^+

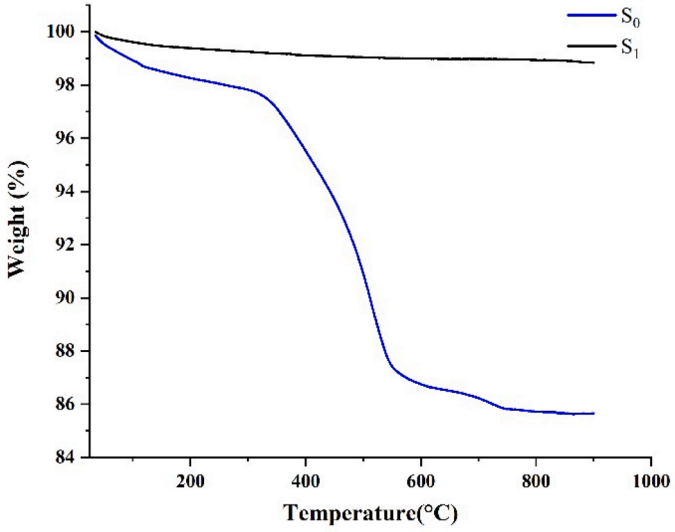

Fig. 8. TGA analysis for Araba Ayachaa shales (S_0) and nano silica (S_1).

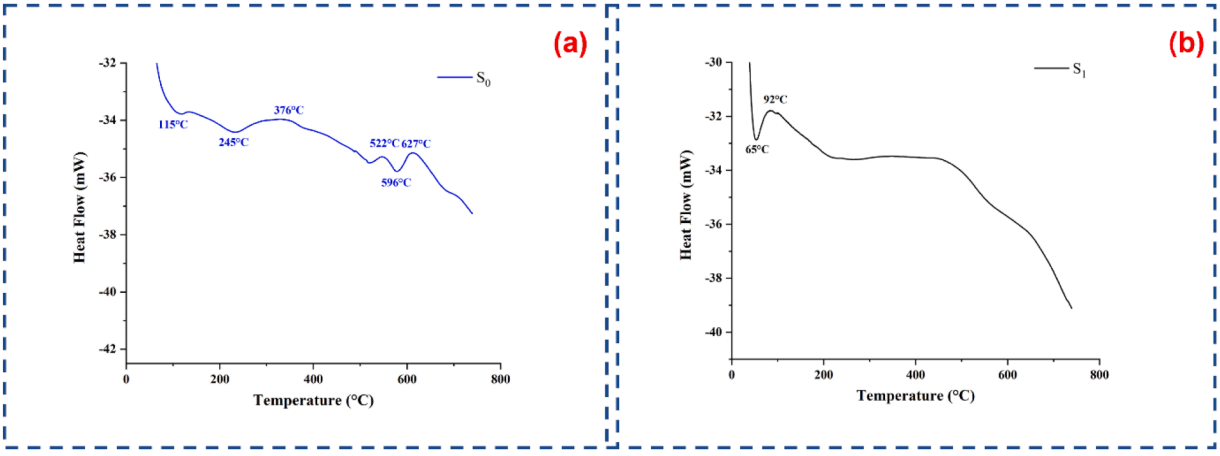

Fig. 7. DSC analysis for Araba Ayachaa shales (a) and nano silica (b).

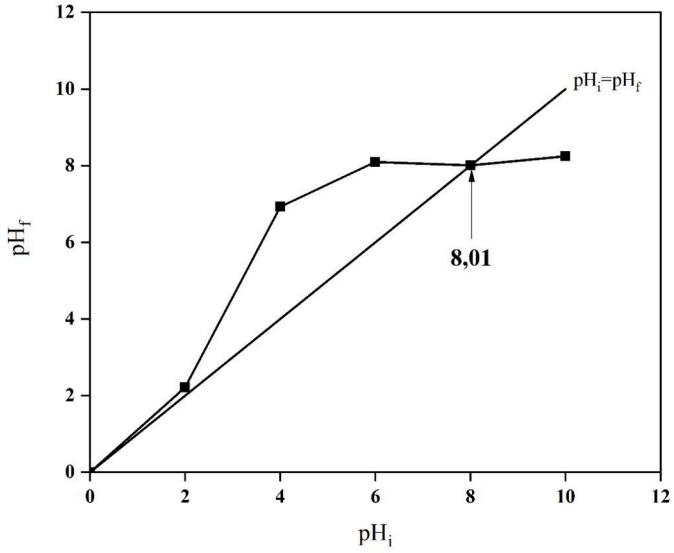

Fig. 9. Determination of the pH_{PZC} of nanosilica powder.

ions [55]. However, due to the presence of OH^- ions, it becomes negatively charged above 8.01 ($pH_{PZC} < pH$).

3.9. Industrial scale-up of nano-silica from Moroccan oil shale: challenges, opportunities, and the role of digital strategies

Subsequent to the laboratory-scale characterization, it is of paramount importance to critically assess the wider industrial and technological implications of this study. While the extracted nano-silica exhibits promising purity, structural stability, and nanoscale characteristics for industrial applications, the reliance on analytical-grade reactants and small-scale laboratory settings restricts the immediate applicability of these findings to real-world manufacturing. Therefore, commercial scale-up must be approached with caution. For a complete evaluation of this method's practicality, it is essential to conduct further studies that take into account several factors starting with the geological heterogeneity of the raw Moroccan oil shale a consequence of its mineral composition, depositional environment, and regional geochemical conditions which determine the extraction yield as well as the product consistency. Moreover, calcination temperature, reaction duration, and acid concentration are key processing parameters that are likely to have a substantial impact on the material's surface area, porosity, and functional group distribution. It is at this juncture that the integration of digital technologies namely generative AI, extended reality (XR), and digital twin simulations, ultimately creates a strategic path that holds significant potential to accelerate process optimization. As evidenced in research by Klieštik et al. [56]. Leveraging AI-driven simulations and data analytics enables the refinement of extraction parameters, prediction of material performance, and modeling of real-world outcomes, resulting in more efficient and commercially viable production approaches. These AI platforms also assist with real-time decision-making, process control, and techno-economic forecasting, bridging the gap between laboratory research and industrial deployment, particularly in resource-limited areas. Building on these advancements, the potential of nano-silica can be further expanded for broader applications, with examples in fields such as agriculture and food, so long as it meets safety and regulatory standards across various regions. Coupling it with biochar could generate novel solutions for environmental remediation, civil engineering and agriculture, such as revolutionizing lightweight concrete production and amplifying fertilizer efficiency, alongside aiding in the reduction of greenhouse gas emissions [57,58]. This work collectively confirms the feasibility of transforming oil shale into valuable nanomaterials while simultaneously driving digital and industrial progress, particularly benefiting resource-limited regions seeking sustainable material production.

4. Conclusion

The production of high-purity amorphous nano-silica ratifies the usefulness of Moroccan oil shale as an efficient precursor. The underexploited shale deposit was successfully converted into a valued nanomaterial (silica nanoparticle), which is consistent with the premise that each shale deposit can be valorized for economic gain via a simple chemical procedure.

According to the findings, this implemented method aligns with the sustainability goals by cutting back on the use of high-energy or imported sources of silica while also exhibiting the performance on par commercial benchmarks. Industrially, this hypostasis offers a cost-effective alternative for the large-scale synthesis of nano-silica, notably in various domains (agriculture, environmental remediation and heterogeneous catalysis). Furthermore, it unlocks new research pathways for developing countries to produce advanced nanomaterial environmental remediation with reduced financial and ecological impact.

Ethical approval

Authors state that the research was conducted according to ethical standards.

Consent to participate

Not applicable.

Consent to publish

Not applicable.

Funding

This research received no external funding.

CRediT authorship contribution statement

Anas Krime: Writing – review & editing, Writing – original draft, Investigation, Formal analysis, Conceptualization. **Miriam Rita Eloufir:** Writing – review & editing. **Sanaâ Saoiabi:** Writing – review & editing, Supervision, Methodology, Investigation, Conceptualization. **Mouhaydine Tlemcani:** Writing – review & editing, Validation, Supervision, Investigation, Conceptualization. **Manuela Morais:** Writing – review & editing, Investigation. **Ahmed Saoiabi:** Validation, Methodology.

Declaration of competing interest

The authors declare the following financial interests/personal relationships which may be considered as potential competing interests:

Mouhaydine Tlemcani has patent #Extraction écologique de nanosilice de haute pureté des schistes bitumineux (68,119) pending to 68119. If there are other authors, they declare that they have no known competing financial interests or personal relationships that could have appeared to influence the work reported in this paper.

Acknowledgments

The authors would like to thank the Centre national de la recherche scientifique et technique and the National Hydrocarbons and Mining Office for their support for this project.

Data availability

Data will be made available on request.

References

[1] C.D. Dominic, N.KV Midhun, P.M. Sabura Begum, R. Joseph, D.dosS. Rosa, Y. Duan, A. Balan, T.G. Ajithkumar, M. Soumya, A. Shelke, J. Parameswaranpillai, M. Badawi, Nanosilica from Averrhoa Bilimbi juice pre-treated rice husk: preparation and characterization, J. Clean. Prod. 413 (2023) 137476, https://doi.org/10.1016/J.JCLEPRO.2023.137476.

[2] J. Maroušek, A. Marouškova, R. Periakaruppan, G.M. Gokul, A. Anbukumaran, A. Bohatá, P. Kříž, J. Bárta, P. Černý, P. Olšan, Silica nanoparticles from Coir pith synthesized by acidic sol-gel method improve germination economics, Polym. (Basel) 14 (2) (2022) 266, https://doi.org/10.3390/POLYM14020266.

[3] R. Ghamarpoor, M. Jamshidi, D.M. Kandelousi, Electromagnetic interference (EMI) shielding, electrical, thermal, and mechanical properties of silanized hexagonal boron nitride (h-BN) heterostructures and decorated by Ag nanoparticles: towards smart coatings, J. Alloy. Compd. 1020 (2025) 179561, https://doi.org/10.1016/J.JALLCOM.2025.179561.

[4] M. Neshastehgar, M. Jamshidi, R. Ghamarpoor, Self-assembly TiO_2@Silane@SiO_2 core-shell as s-scheme heterojunction photocatalyst against methylene blue degradation: synthesis and mechanism insights, J. Mol. Struct. 1319 (2025) 139406, https://doi.org/10.1016/J.MOLSTRUC.2024.139406.

[5] R. Ghamarpoor, M. Jamshidi, A. Fallah, M. Neshastehgar, Designing a smart acrylic photocatalyst coating loaded with N/C-doped TiO_2@SiO_2 core-shell by bio-based Tarem-rice husk waste for organic pollutant degradation, Alexand. Eng. J. 115 (2025) 131–146, https://doi.org/10.1016/J.AEJ.2024.12.023.

[6] A.B. Prasetyo, M. Handayani, E. Sulistiyono, F. Firdiyono, E. Febriana, W. Mayangsari, S. Wahyuningsih, E. Pramono, A. Maksum, R. Riastuti, J. W. Soedarsono, Fabrication of high purity silica precipitates from quartz sand toward photovoltaic application, J. Ceram. Process. Res. 24 (1) (2023) 103–110, https://doi.org/10.36410/JCPR.2023.24.1.103.

[7] F. Akhter, A.R. Jamali, W. Khan, TEOS-doped vs non-TEOS silica aerogels: a comparative study of synthesis, characterization, isotherm studies and performance evaluation for Pb (II) removal from synthetic wastewater, Water Air Soil Pollut. 234 (1) (2023) 1–9, https://doi.org/10.1007/S11270-022-06051-4/TABLES/3.

[8] J. Maroušek, Y. Kawamitsu, M. Ueno, Y. Kondo, L. Kolář, Methods for improving methane yield from rye straw, Appl. Eng. Agric. 28 (5) (2012) 747–755, https://doi.org/10.13031/2013.42417.

[9] J.. Maroušek, Study on commercial scale steam explosion of winter brassica napus STRAW, Int. J. Green Energy 10 (9) (2013) 944–951, https://doi.org/10.1080/15435075.2012.732158.

[10] M. Akbari, N. Loganathan, H. Tavakolian, A. Mardani, D. Streimikiene, The dynamic effect of micro-structural shocks on private investment behavior /, Acta Montanist. Slov. 26 (1) (2021) 1–17, https://doi.org/10.46544/AMS.V26I1.01.

[11] S. Saoiabi, S. Latifi, A. Gouza, L.E. Hammari, O. Boukra, A. Saoiabi, Elimination of heavy metal Ni2+ from wastewater using Moroccan oil shale as bio sorbent, Mater. Today: Proceed. 58 (2022) 987–993, https://doi.org/10.1016/J.MATPR.2021.12.457.

[12] H. Majdoubi, S. Şimşek, R.E.K. Billah, N. Koçak, S. Kaya, Y. Tamraoui, K.P. Katin, H. Hannache, R. Marzouki, Novel geopolymer composite based on oil shale and chitosan for enhanced uranium (VI) adsorption: experimental and theoretical approaches, J. Mol. Liq. 395 (2024) 123951, https://doi.org/10.1016/J.MOLLIQ.2024.123951.

[13] Anon, Adsorption of organic pollutants using Moroccan oil shales: optimization of the Adsorption process using a factorial design, NanoWorld J. 9 (2023), https://doi.org/10.17756/NWJ.2023-S2-067.

[14] P. Sharma, J. Prakash, R. Kaushal, An insight into the green synthesis of SiO_2 nanostructures as a novel adsorbent for removal of toxic water pollutants, Environ. Res. 212 (2022) 113328, https://doi.org/10.1016/J.ENVRES.2022.113328.

[15] J.Y. Park, Y.M. Gu, S.Y. Park, E.T. Hwang, B.I. Sang, J. Chun, J.H. Lee, Two-stage continuous process for the extraction of silica from rice husk using attrition ball milling and alkaline leaching methods, Sustainability 13 (13) (2021) 7350, https://doi.org/10.3390/SU13137350.

[16] A. Ganguli, A. Ganguly, Highly uniform nano and mesostructures of silica obtained by reverse micellar and hydrothermal methods, J. Clust. Sci. 20 (2) (2009) 417–427, https://doi.org/10.1007/S10876-009-0255-4/FIGURES/7.

[17] X. Ying-Mei, Q. Ji, S. Jia-Wei, H. De-Min, W. Dong-Mei, Z. Zhang, Technique of preparing modified silica from oil shale residue, Oil Shale 28 (2) (2011) 309, https://doi.org/10.3176/OIL.2011.2.05.

[18] K. Durairaj, P. Senthilkumar, P. Velmurugan, K. Dhamodaran, K. Kadirvelu, S. Kumaran, Sol-gel mediated synthesis of silica nanoparticle from Bambusa Vulgaris leaves and its environmental applications: kinetics and isotherms studies, J. Solgel. Sci. Technol. 90 (3) (2019) 653–664, https://doi.org/10.1007/S10971-019-04922-7/FIGURES/7.

[19] R.A. Bakar, R. Yahya, S.N. Gan, Production of high purity amorphous silica from rice husk, Procedia Chem. 19 (2016) 189–195, https://doi.org/10.1016/J.PROCHE.2016.03.092.

[20] G. Falk, G.P. Shinhe, L.B. Teixeira, E.G. Moraes, A.P. Novaes de Oliveira, Synthesis of silica nanoparticles from sugarcane bagasse ash and nano-silicon via magnesiothermic reactions, Ceram. Int. 45 (17) (2019) 21618–21624, https://doi.org/10.1016/J.CERAMINT.2019.07.157.

[21] P. Pillai, S. Dharaskar, M. Shah, R. Sultania, Determination of fluoride removal using silica nano adsorbent modified by rice husk from water, Groundw. Sustain. Develop. 11 (2020) 100423, https://doi.org/10.1016/J.GSD.2020.100423.

[22] S. Mor, C.K. Manchanda, S.K. Kansal, K. Ravindra, Nanosilica extraction from processed agricultural residue using green technology, J Clean Prod 143 (2017) 1284–1290, https://doi.org/10.1016/J.CLEPRO.2016.11.142.

[23] A.L.K. Groune, A.L.K. Groune, Mineralogical properties of Moroccan Rif bituminous rocks. Recent Advances in Mineralogy, 2023, https://doi.org/10.5772/INTECHOPEN.112710.

[24] R. Zhao, N. Xiao, Y. Liu, W. Zhan, Z. Wu, Study on extraction of silica from rice husk by sol–Gel method and its application in catalytic decomposition of methane, Biomass Convers. Biorefin. 14 (9) (2024) 10067–10083, https://doi.org/10.1007/S13399-022-03180-Y/TABLES/1.

[25] R. Kamboj, A. Bains, M. Sharma, A. Kumar, N. Ali, M. Khalid Parvez, P. Chawla, K. Sridhar, Green synthesis of rice straw-derived silica nanoparticles by hydrothermal process for antimicrobial properties and effective degradation of dyes, Process Safet. Environ. Protect. 185 (2024) 1049–1060, https://doi.org/10.1016/J.PSEP.2024.03.078.

[26] A. Ouallali, M. Moukhchane, H. Aassoumi, F. Berrad, I. Dakir, The mapping of the soils' degradation state by adaptation the PAP/RAC guidelines in the watershed of Wadi Arbaa Ayacha, Western Rif, Morocco, J. Geosci. Environ. Protect. 04 (07) (2016) 77–88, https://doi.org/10.4236/GEP.2016.47009.

[27] L. Xu, J. Zhang, J. Ding, T. Liu, G. Shi, X. Li, W. Dang, Y. Cheng, R. Guo, Pore structure and fractal characteristics of different shale lithofacies in the Dalong Formation in the western area of the lower Yangtze Platform, Minerals 10 (1) (2020) 72, https://doi.org/10.3390/MIN10010072.

[28] T.T. Nguyen, H.T. Ma, P. Avti, M.J.K. Bashir, C.A. Ng, L.Y. Wong, H.K. Jun, Q. M. Ngo, N.Q. Tran, Adsorptive removal of iron using SiO_2 nanoparticles extracted from rice husk ash, J. Anal. Method. Chem. 2019 (1) (2019) 6210240, https://doi.org/10.1155/2019/6210240.

[29] N. Gautam, Y. Rajesh, N. Kale, M. Jagtap, H. Chaudhari, S. Pansare, Silica extraction from bamboo leaves using alkaline extraction method, in: Materials Today: Proceedings, 2023, https://doi.org/10.1016/J.MATPR.2023.12.014.

[30] F. Farirai, M. Mupa, M.O. Daramola, An improved method for the production of high purity silica from sugarcane bagasse ash obtained from a bioethanol plant boiler, Particul. Sci. Technol. 39 (2) (2021) 252–259, https://doi.org/10.1080/02726351.2020.1734700;WEBSITE:WEBSITE:TFOPB;JOURNAL:JOURNAL:UPST20;PAGEGROUP:STRING:PUBLICATION.

[31] Z.A.S.A. Salim, H. Ismail, A. Hassan, N.H.C. Ismail, F. Hashim, Characterisation of high purity rice Husk Silica synthesised using solvent-thermal treatment with different concentration of acid leaching, Jurnal Teknologi (Sci. Eng.) 85 (2) (2023) 101–110, https://doi.org/10.11113/JURNALTEKNOLOGI.V85.18631.

[32] S. Silviana, F. Dalanta, G.J. Sanyoto, Utilization of bamboo leaf silica as a superhydrophobic coating using trimethylchlorosilane as a surface modification agent, J. Phys.: Conferen. Ser. 1943 (1) (2021) 012180, https://doi.org/10.1088/1742-6596/1943/1/012180.

[33] R. Ghamarpoor, M. Jamshidi, Preparation of superhydrophobic/superoleophilic nitrile rubber (NBR) nanocomposites contained silanized nano silica for efficient oil/water separation, Sep. Purif. Technol. 291 (2022) 120854, https://doi.org/10.1016/J.SEPPUR.2022.120854.

[34] E.C. Peres, J.C. Slaviero, A.M. Cunha, A. Hosseini-Bandegharaei, G.L. Dotto, Microwave synthesis of silica nanoparticles and its application for methylene blue adsorption, J. Environ. Chem. Eng. 6 (1) (2018) 649–659, https://doi.org/10.1016/J.JECE.2017.12.062.

[35] E.B. Ekwenna, Y. Wang, A. Roskilly, The production of bio-silica from Agro-industrial wastes leached and anaerobically digested rice straws, Bioresour. Technol. Rep. 22 (2023) 101452, https://doi.org/10.1016/J.BITEB.2023.101452.

[36] N. Yekeen, S.N. Salampessy, A.H.A. Bakar, M. Ali, O.A. Okunade, S.A. Musa, C. B. Bavoh, Synthesis and pore-scale visualization studies of enhanced oil recovery mechanisms of rice straw silica nanoparticles, Geoenergy Sci. Eng. 221 (2023) 111292, https://doi.org/10.1016/J.PETROL.2022.111292.

[37] N. El Messaoudi, M.E. Khomri, A.B. El Houssaine Ablouh, A. Lacherai, A. Jada, E. C. Lima, F. Sher, Biosynthesis of SiO_2 nanoparticles using extract of nerium oleander leaves for the removal of tetracycline antibiotic, Chemosphere 287 (2022) 132453, https://doi.org/10.1016/J.CHEMOSPHERE.2021.132453.

[38] T. Qian, J. Li, H. Ma, J. Yang, The preparation of a green shape-stabilized composite phase change material of polyethylene glycol/SiO_2 with enhanced thermal performance based on oil shale ash via temperature-assisted sol–Gel method, Sol. Energy Mater. Sol. Cell. 132 (2015) 29–39, https://doi.org/10.1016/J.SOLMAT.2014.08.017.

[39] I. Kouadri, B. Ben Seghir, H. Hemmami, S. Zeghoud, N. Allag, A. Rebiai, I. Ben Amor, A. Chala, H. Belkhalfa, Extraction of silica from different sources of agricultural waste, Asia. J. Res. Chem. (2023) 97–101, https://doi.org/10.52711/0974-4150.2023.00016.

[40] P. Karo-Karo, S. Sembiring, I. Firdaus, R. Situmeang, S.D. Yuwono, Preparation of silver-doped rice husk silica composites using the sol-gel method, Ceram. - Silikaty 66 (3) (2022) 365–373, https://doi.org/10.13168/CS.2022.0032.

[41] E.C. Moine, R. Bouamoud, A. El Hamidi, M. Khachani, M. Halim, S. Arsalane, Mineralogical characterization and non-isothermal pyrolysis kinetics of Moroccan Rif Oil shale, J. Therm. Anal. Calorim. 131 (2) (2018) 993–1004, https://doi.org/10.1007/S10973-017-6632-6/TABLES/6.

[42] P.E. Imoisili, K.O. Ukoba, T.C. Jen, Synthesis and characterization of amorphous mesoporous silica from palm kernel shell ash, Boletín de La Sociedad Española de Cerámica y Vidrio 59 (4) (2020) 159–164, https://doi.org/10.1016/J.BSECV.2019.09.006.

[43] S. Salakhum, T. Yutthalekha, M. Chareonpanich, J. Limtrakul, C. Wattanakit, Synthesis of hierarchical faujasite nanosheets from corn cob ash-derived nanosilica as efficient catalysts for hydrogenation of lignin-derived alkylphenols, Micropor. Mesopor. Mater. 258 (2018) 141–150, https://doi.org/10.1016/J.MICROMESO.2017.09.009.

[44] K. Groune, M. Halim, S. Arsalane, Thermal and mineralogical studies of Moroccan rif bituminous rocks, Oil Shale 30 (4) (2013) 536–549, https://doi.org/10.3176/OIL.2013.4.06.

[45] A. Mourhly, F. Jhilal, A.E. Hamidi, M. Halim, S. Arsalane, Highly efficient production of mesoporous nano-silica from unconventional resource: process optimization using a Central composite design, Microchem. J. 145 (2019) 139–145, https://doi.org/10.1016/J.MICROC.2018.10.030.

[46] V.K. Yadav, M.H. Fulekar, Green synthesis and characterization of amorphous silica nanoparticles from fly ash, Mater. Today: Proceed. 18 (2019) 4351–4359, https://doi.org/10.1016/J.MATPR.2019.07.395.

[47] Q.V. Bach, C.M. Vu, H.T. Vu, Effects of Co-silanized silica on the mechanical properties and thermal characteristics of natural rubber/styrene-butadiene rubber blend, Silicon 12 (8) (2020) 1799–1809, https://doi.org/10.1007/S12633-019-00281-8/METRICS.

[48] J. Cao, J. Wang, X. Wang, J. Zhang, K. Liu, Y. Wang, W. Zhen, Y. Chen, Preparation and characterization of modified amphiphilic nano-silica for enhanced oil recovery, Colloid. Surf. A: Physicochem. Eng. Asp. 633 (2022) 127864, https://doi.org/10.1016/J.COLSURFA.2021.127864.

[49] B. Rojek, A. Bartyzel, W. Sawicki, A. Plenis, DSC, TGA-FTIR and FTIR assisted by chemometric factor analysis and PXRD in assessing the incompatibility of the antiviral drug arbidol hydrochloride with pharmaceutical excipients, Molecules 29 (1) (2024) 264, https://doi.org/10.3390/MOLECULES29010264.

[50] Z. Li, L. Cui, B. Li, X. Du, Effects of SiO2 nanoparticle dispersion on the heat storage property of the solar salt for solar power applications, Energies 14 (3) (2021) 703, https://doi.org/10.3390/EN14030703.

[51] Y. Miyah, A. Lahrichi, M. Idrissi, S. Boujraf, H. Taouda, F. Zerrouq, Assessment of adsorption kinetics for removal potential of crystal violet dye from aqueous solutions using Moroccan pyrophyllite, J. Assoc. Arab Universit. Bas. Appl. Sci. 23 (2017) 20–28, https://doi.org/10.1016/J.JAUBAS.2016.06.001.

[52] Y. Miyah, A. Lahrichi, M. Idrissi, A. Khalil, F. Zerrouq, Adsorption of methylene blue dye from aqueous solutions onto walnut shells powder: equilibrium and kinetic studies, Surface. Interface. 11 (2018) 74–81, https://doi.org/10.1016/J.SURFIN.2018.03.006.

[53] S.T. Al-Asadi, Z.H. Mussa, F.F. Al-Qaim, H. Kamyab, H.F.S. Al-Saedi, I.F. Deyab, N. J. Kadhim, A comprehensive review of methylene blue dye adsorption on activated carbon from edible fruit seeds: a case study on kinetics and adsorption models, Carb. Trend. 20 (2025) 100507, https://doi.org/10.1016/J.CARTRE.2025.100507.

[54] S. He, Q. Chen, G. Chen, G. Shi, C. Ruan, M. Feng, Y. Ma, X. Jin, X. Liu, C. Du, C. He, H. Dai, C. Cao, N-doped activated carbon for high-efficiency ofloxacin adsorption, Micropor. Mesopor. Mater. 335 (2022) 111848, https://doi.org/10.1016/J.MICROMESO.2022.111848.

[55] A. Thakur, N. Sharma, A. Mann, Removal of ofloxacin hydrochloride and paracetamol from aqueous solutions: binary mixtures and competitive adsorption, Mater. Today: Proceed. 28 (2020) 1514–1519, https://doi.org/10.1016/J.MATPR.2020.04.833.

[56] Anon, Generative artificial intelligence of things systems, multisensory immersive extended reality technologies, and algorithmic big data simulation and modelling tools in digital twin industrial metaverse, Equilibr. Q. J. Econ. Econ. Policy 19 (2) (2024) 429–461.

[57] J. Marousek, B. Gavurova, A. Marouskova, B. Minofar, Techno-economic aspects of concrete lightweighting by char enrichment with phosphates from wastewater, Chem. Eng. J. Adv. 22 (2025) 100712, https://doi.org/10.1016/J.CEJA.2025.100712.

[58] B. Minofar, N. Milčić, J. Maroušek, B. Gavurová, A. Marouśková, Understanding the molecular mechanisms of interactions between biochar and denitrifiers in N_2O emissions reduction: pathway to more economical and sustainable fertilizers, Soil Tillage Res. 248 (2025) 106405, https://doi.org/10.1016/J.STILL.2024.106405.